Heteroepitaxially Grown Zeolitic Imidazolate Framework Membranes with Unprecedented Propylene/Propane Separation Performances

Hyuk Taek Kwon,[†] Hae-Kwon Jeong,*[,†,‡] Albert S. Lee,[‡] He Seong An,[§,‖] and Jong Suk Lee[‖]

[†]Artie McFerrin Department of Chemical Engineering and [‡]Department of Materials Science and Engineering, Texas A&M University, 3122 TAMU, College Station, Texas 77843-3122, United States

[‡]Materials Architecturing Research Center, Korea Institute of Science and Technology, Hwarang-ro 14-gil, Seongbuk-gu, Seoul 136-791, Republic of Korea

[§]Department of Chemical and Biological Engineering, Korea University, 5-1 Anam-dong, Seongbuk-gu, Seoul 136-713, Republic of Korea

[‖]Center for Environment, Health and Welfare Research, Korea Institute of Science and Technology, Hwarang-ro 14-gil, Seongbuk-gu, Seoul 136-791, Republic of Korea

S *Supporting Information*

ABSTRACT: Propylene/propane separation is one of the most challenging separations, currently achieved by energy-intensive cryogenic distillation. Despite the great potential for energy-efficient membrane-based separations, no commercial membranes are currently available due to the limitations of current polymeric materials. Zeolitic imidazolate framework, ZIF-8, with the effective aperture size of ~4.0 Å, has been shown to be very promising for propylene/propane separation. Despite the extensive research on ZIF-8 membranes, only a few reported ZIF-8 membranes have displayed good propylene/propane separation performances presumably due to the challenges of controlling the microstructures of polycrystalline membranes. Here we report the first well-

intergrown membranes of ZIF-67 (Co-substituted ZIF-8) by heteroepitaxially growing ZIF-67 on ZIF-8 seed layers. The ZIF-67 membranes exhibited impressively high propylene/propane separation capabilities. Furthermore, when a tertiary growth of ZIF-8 layers was applied to heteroepitaxially grown ZIF-67 membranes, the membranes exhibited unprecedentedly high propylene/propane separation factors of ~200 possibly due to enhanced grain boundary structure.
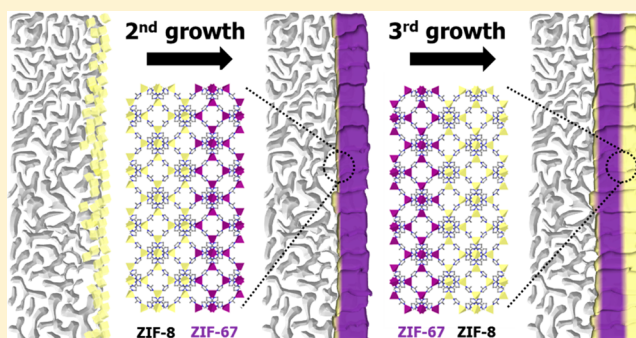
INTRODUCTION

Propylene is one of the most highly demanded commodity chemicals in the chemical and petrochemical industries. When produced by the steam-cracking of hydrocarbon sources such as natural gas, propylene needs to be separated from propane. Currently highly energy-intensive cryogenic distillation is employed due to the similar physical properties (e.g., volatility and size) between propane and propylene. Despite tremendous research interests in more energy-efficient membrane-based separation technologies, there exist no commercial membranes currently available for propylene/propane separation mainly due to the limitations of polymeric membranes (i.e., low separation factor).[1,2] Though molecular sieving materials such as carbon molecular sieves[3−6] and zeolites[7] are shown to be promising, the majority of these materials fail to meet the performance requirements except for a few.[1,8] Facilitated transport membranes[9] exhibit extremely high separation factors but suffer from irreversible degradation due to the impurities in the feed stream.

Due to their well-defined pores and labile surface chemistry, MOFs have drawn tremendous attentions as a new class of membrane materials for gas/liquid separations.[10−12] Zeolitic imidazolate frameworks (ZIFs)[13] with zeolite topologies, consisting of transition metals (Zn or Co) and imidazole-based ligands, are of particular interest and are most extensively investigated for membrane-based gas separations[14] mainly owing to their ultramicropores and relatively high thermal/chemical stabilities as compared to other MOFs.[13] To date, several ZIF materials such as ZIF-7,[15] ZIF-8,[16] ZIF-22,[17] ZIF-69,[18] ZIF-71,[19] ZIF-78,[20] ZIF-90,[21] ZIF-95,[22] and SIM-1[23] have been successfully processed into supported polycrystalline and/or mixed matrix membranes and tested for gas separations.[14] Due to the effective aperture of ~4.0 Å,[24] ZIF-8 membranes showed a sharp propylene/propane separation based on size exclusion principle.[8,25−32] So far, well-intergrown ZIF-8 membranes were prepared using either *in situ*[8,16,33] or
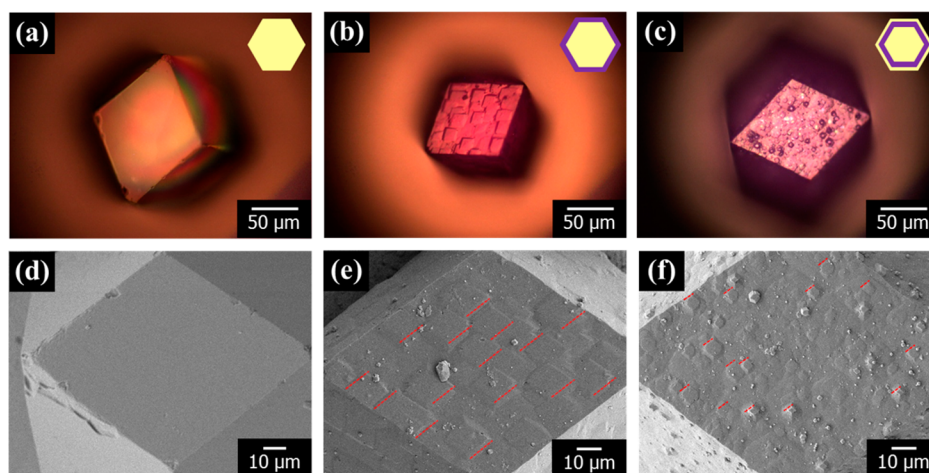
Figure 1. Optical and electron micrographs of the {110} facets of a ZIF-8 single crystal (a, d), a ZIF-8@ZIF-67 core−shell (b, e), and a ZIF-8@ZIF-67@ZIF-8 core−shell (c, f). A, B, C in an A@B@C structure indicates that a core crystal, a second subshell, and the most outer shell, respectively.

secondary[26−28,34] growth. However, only a few ZIF-8 membranes[8,23,25−31] exhibited relatively high propylene/propane separation performances primarily because of the difficulty in controlling the microstructures of polycrystalline membranes (e.g., grain boundary structure). It is noted that the separation performance of well-intergrown polycrystalline ZIF-8 membranes is determined not only by the selective intracrystalline diffusion (i.e., intrinsic material property) but also by the nonselective intercrystalline diffusion (i.e., grain boundary structure). This is equivalent to the resistances-in-parallel model where the overall transport resistance is governed by the relative importance of the two transport resistances, one through grains and the other through grain boundaries. The microstructures of polycrystalline films are greatly affected by processing techniques. It is, therefore, imperative to develop new processing techniques that may result in the improved microstructures of polycrystalline membranes, thereby leading to the improved separation performances.

Heteroepitaxial growth is an effective strategy to engineer the properties of crystalline materials by combining different crystalline systems via molecular-level connections. As opposed to other MOF modification strategies (e.g., metal/ligand exchange and covalent/click chemistry on ligand pendent groups),[35] this molecular-level connection between two different crystalline systems enables the formation of hybrid crystals possessing combined properties without sacrificing the intrinsic features of individual crystals.[36] This unique advantage of heteroepitaxial growth resulted in a battery of hierarchical MOF structures[37−47] which cannot be obtained otherwise.[35] Kitagawa and his co-workers constructed hybrid MOF structures such as heterometallic core−shells,[38] ABA-type blocks,[39] and hybrid oriented films,[42] and shed light on the epitaxial relations via exhaustive surface X-ray diffraction analyses.[38,39,42] Later, several groups reported heteroepitaxially grown hybrid MOFs including IRMOF-1/-3 core−shells,[40,44,47] hybrid SURMOFs using [Cu$_2$(bdc)$_2$(dabco)], [Cu$_2$(NH$_2$-bdc)$_2$(dabco)], and [Cu$_2$(ndc)$_2$(dabco)],[41] and more recently ZIF-67/-8 Janus crystals.[45] Furthermore, in our previous report,[47] we demonstrated that IRMOF-3/IRMOF-1 hybrid membranes can be prepared by heteroexpitaxially growing IRMOF-3 on IRMOF-1 seed crystal layers. It should be noted that several zeolite films and membranes were also prepared using the heteroepitaxial growth strategy.[48,49] To the best of

our knowledge, there have been no reported ZIF membranes prepared by the heteroepitaxial growth.

ZIF-67 is a cobalt-substituted equivalent to ZIF-8 composed of cobalt ions interconnected with 2-methylimidazole ligand,[50] forming a SOD zeolite topology. Since it is isostructural to ZIF-8, we reckoned ZIF-67 membranes might be promising for propylene/propane separation as with ZIF-8 membranes.[8,25−31] In addition, due to the presence of the redox catalytic cobalt centers,[51−56] ZIF-67 membranes have the potential to be effective perm-selective membrane reactors. To the best of our knowledge, however, there has been no report on well-intergrown ZIF-67 membranes.

To this end, we report the first ZIF-67 membranes, exhibiting excellent propylene/propane separation performances. Submicron-thick ZIF-67 membranes were heteroepitaxially grown from ZIF-8 seed layers. The heteroepitaxy between ZIF-8 and ZIF-67 was unambiguously determined by constructing core−shells such as ZIF-8@ZIF-67 (ZIF-67 shell on ZIF-8 core) and ZIF-8@ZIF-67@ZIF-8 (ZIF-8 shell on ZIF-8@ZIF-67 core−shell) and observing the growth of shell layers that preserved both in-plane and out-of-plane orientations. Furthermore, a tertiary heteroepitaxial growth of ZIF-8 layers on ZIF-67 membranes turned out to be an effective means to further improve membrane microstructures, leading to significant enhancement in propylene/propane separation factors.

■ RESULTS AND DISCUSSION

Establishment of Heteroepitaxy. ZIF-8 and ZIF-67 are isostructural (i.e., crystallographically the same structure) with different metal nodes (Zn in ZIF-8 and Co in ZIF-67). They share the same crystallographic features such as crystal system and space group with similar lattice parameters [cubic, $I\bar{4}3m$, and a = 16.881 Å (ZIF-8)/16.908 Å (ZIF-67) at 110 K (see Table S1)]. It is, therefore, expected that we would obtain the heteroepitaxial growth of these two isostructural ZIFs. It should be pointed out that, while preparing this manuscript, two independent reports were brought to our attention, showing ZIF-67/-8 Janus crystals[45] and ZIF-8@ZIF-67 core−shell structures,[57] respectively. None of these reports, however, presented unambiguous evidence of heteroepitaxial growth.

To establish the heteroepitaxial relationships between ZIF-8 and ZIF-67, core−shell structures of ZIF-8@ZIF-67 and ZIF-
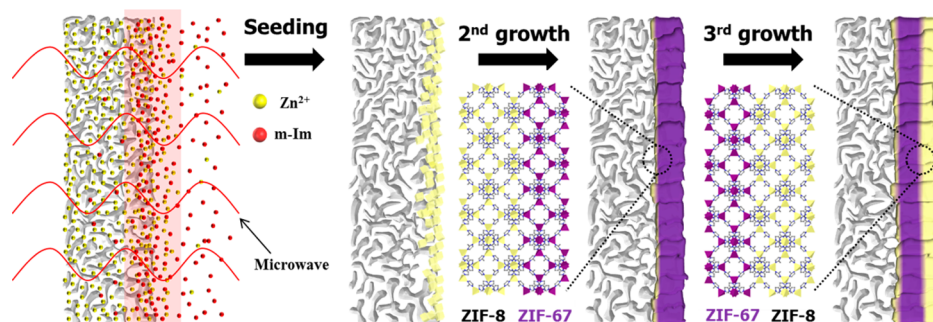
Figure 2. Schematic illustration of the membrane synthesis via heteroepitaxial growth.
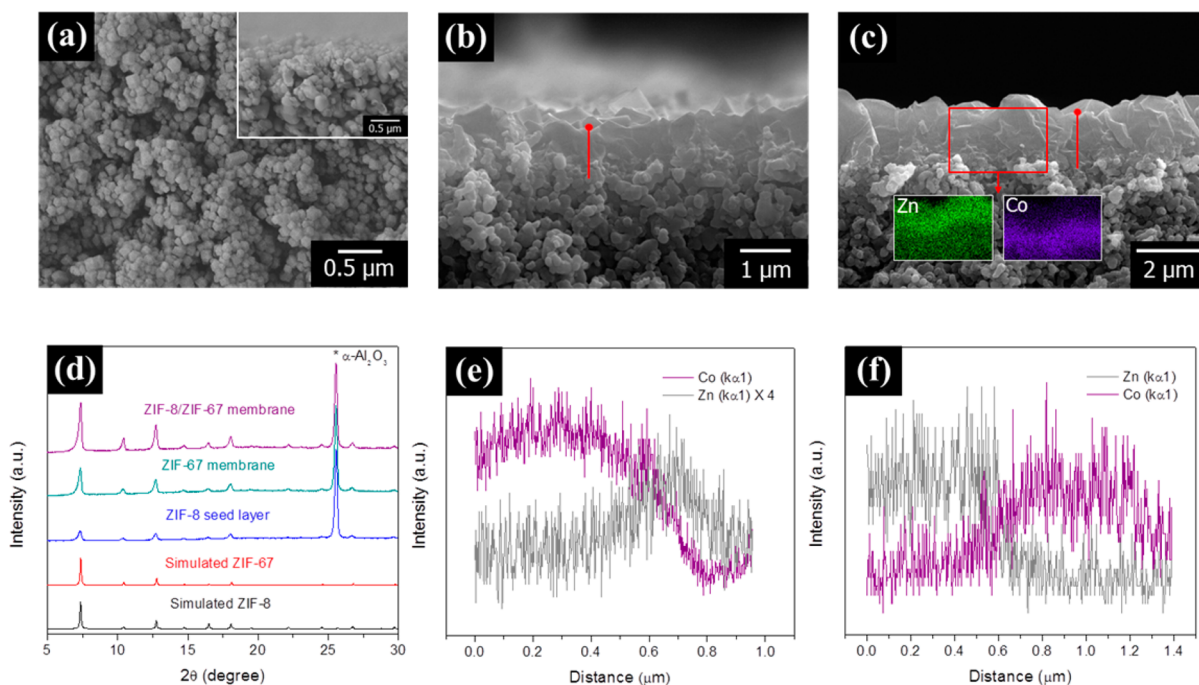

Figure 3. Electron micrographs of a ZIF-8 seed layer (a), a ZIF-67 membrane (b), and a ZIF-8/ZIF-67 membrane (c); X-ray diffraction patterns of the ZIF-8 seed layer, ZIF-67, and ZIF-8/ZIF-67 membrane (d); energy-dispersive X-ray elemental profiles of the cross section of the ZIF-67 (e) and ZIF-8/ZIF-67 membranes (f) with the corresponding red solid lines marked in parts b and c. The inset image in part a shows the cross-sectional view of the seed layer.

8@ZIF-67@ZIF-8 were prepared solvothermally. Figure 1 presents optical and electron micrographs of the core–shell structures. It should be noted that the colors of the samples are different from those under the optical microscope due to an optical filter. ZIF-67 and ZIF-8 powders are in purple and in yellow, respectively, as shown in Figure S1. As-synthesized core ZIF-8 single crystals have a rhombic dodecahedron shape with 12 of the {110} facets with size ca. 150 μm. The ZIF-8 core crystals are transparent with a yellowish tint and have relatively smooth surfaces (Figure 1a,d). Upon growing a ZIF-67 shell, the crystal exhibits a purplish red color (Figure 1b) and a pinkish red color after the subsequent growth of an additional ZIF-8 layer on ZIF-8@ZIF-67 (Figure 1c), indicating the growth of overlayers on the core crystals. Powder X-ray diffraction patterns of the core–shell crystals confirmed that the samples were phase-pure (see Figure S2a,b). Figure 1e,f presents the electron micrographs of the core–shell samples. As compared to ZIF-8 core crystals (Figure 1d), newly grown shell crystal domains are observed on the external surfaces of both core–shell crystals. These domains have a rhombus shape

resembling the shape of the {110} facets of ZIF-8 core crystals. As highlighted with red dotted lines marked on the electron micrographs, individual domains are aligned with each other along the in-plane directions as well as with core crystals, explicitly confirming that the shells were grown in an epitaxial manner.[45] Individual shell domains of ZIF-8@ZIF-67 and ZIF-8@ZIF-67@ZIF-8 were compared in Figure S3. As shown, domains were different in size as well as in the level of their shape development. Under the same growth conditions, ZIF-8 shell domains (Figure S3c) were smaller in size and not well-developed along the [−110] direction evidenced by the presence of numerous terraces and steps as compared to ZIF-67 shell domains (Figure S3b). This suggests that, under the current synthesis conditions, ZIF-67 shells nucleate and grow faster than ZIF-8 shells, and the growth of ZIF-8 shells along the [001] direction is faster than along the [−110] direction. Indeed, ZIF-67 grew faster than ZIF-8 as evidenced by the average particle size of powders collected from the growth solutions (∼0.5 μm (ZIF-8) vs ∼1 μm (ZIF-67)) as shown in Figure S4.

Synthesis of ZIF-67 and ZIF-8/ZIF-67 Membranes.
Figure 2 illustrates the heteroepitaxial synthesis of ZIF membranes. In order to prepare well-intergrown ZIF-67 membranes using the heteroepitaxial growth, densely packed ZIF-8 seed crystals were first deposited on α-Al_2O_3 supports using the microwave-assisted seeding method.[26] Subsequently, ZIF-67 crystals were grown on ZIF-8 seed layers in a heteroepitaxial manner. The microwave-assisted seeding method[26] enables to achieve ZIF-8 seed layers rather strongly attached to supports due to the rapid formation of seed crystals with a majority of crystals formed inside supports as presented in Figure 3a. With strongly bound ZIF-8 seed crystals, well-intergrown defect-free ZIF-67 membranes (hereafter, ZIF-67 membranes) with a thickness of ca. 700 nm were produced by heteroepitaxially growing ZIF-67 from ZIF-8 seed crystals (see Figure 3b,d and Figure S5). Figure 3e shows an EDX line scan analysis along the cross-section of ZIF-67 membranes marked with a red solid line. As expected, a zinc-rich region is clearly seen as moving to the bottom of the membranes, ca. 700 nm in depth, demonstrating the presence of ZIF-8 seed crystals embedded in the membrane structure and the continuous growth of the ZIF-67 layer from the ZIF-8 seed crystals. Similarly, when additional ZIF-8 layers (hereafter, ZIF-8 overlayers) were overgrown on ZIF-67 membranes (i.e., tertiary growth), the resulting membranes (hereafter, ZIF-8/ZIF-67 membranes) appear to be well-intergrown and grown seamlessly while the thickness of the membranes increased to ca. 1.4 μm (Figure 3c,d). Elemental maps and profiles confirm the presence of a ZIF-8 layer on top of the ZIF-67 layer as shown in Figure 3c,f.

The strong attachment of ZIF-8 seed crystal layers on alumina supports was found to be critical to achieve well-intergrown ZIF-67 membranes. With ZIF-8 seed layers prepared by a simple dip-coating method (Figure S6a), it was not possible to obtain ZIF-67 membranes. Instead, an unknown dense phase with a plate-like morphology was formed on the support (Figure S6b,c). The powder sample that precipitated simultaneously in the solution was, however, determined to be phase-pure ZIF-67 (Figure S7). The same unknown phase was also formed on unseeded alumina supports (Figure S8). On the basis of these observations, it is presumed that the unknown phase was formed, likely catalyzed by α-Al_2O_3 supports under the current synthesis conditions. When weakly attached, seed crystals can be easily detached from the supports during the secondary growth step, failing to form ZIF-67 films, instead resulting in the formation of the unknown phase.

It should be noted that our repeated attempts failed to synthesize high-quality ZIF-67 membranes with ZIF-67 seed layers prepared by the microwave-assisted seeding method mainly due to the poor quality of ZIF-67 seed layers as shown in Figure S9. This is attributed to the fact that ZIF-67 nucleates and grows faster than ZIF-8 under the current synthesis conditions. When crystals nucleate and grow too fast, homogeneous nucleation/growth can be significant relative to heterogeneous nucleation/growth, leading to the poor quality of seed layers.

Propylene/Propane Separation Performances of ZIF-67 Membranes. Due to the very close structural similarities between ZIF-8 and ZIF-67, one might expect a keen kinetic separation of a propylene/propane mixture from ZIF-67 membranes based on the size-exclusion principle as observed in ZIF-8 membranes.[58] It is noteworthy that, as with ZIF-8,[58] ZIF-67 presented a negligible solubility contribution on

propylene/propane separation, evidenced by almost identical propylene/propane adsorption isotherm profiles as shown in Figure S10. The separation performances of heteroepitaxially grown membranes (ZIF-67 and ZIF-8/ZIF-67 membranes) were examined by performing gas separation measurements with a binary (50/50) propylene/propane mixture using a Wicke−Kallenbach setup (Figure S11) under ambient conditions. Table 1 summarizes the performance results of all

Table 1. Room-Temperature Binary Propylene/Propane Separation Performances of ZIF-67, ZIF-8/ZIF-67, and ZIF-67/ZIF-67 Membranes Grown on ZIF-8 Seed Layers[a]

membrane	thickness (μm)	C_3H_6 permeance ($\times 10^{-10}$ mol Pa^{-1} m^{-2} s^{-1})	C_3H_6/C_3H_8 separation factor
ZIF-67	0.7	460.8 ± 56.1	84.8 ± 6.2
ZIF-8/ZIF-67[b]	1.0	370.0 ± 33.7	209.1 ± 8.5
ZIF-67/ZIF-67[b]	1.5	309.0 ± 10.9	163.2 ± 30.9

[a]The average and standard deviation values were calculated from the performances of three membranes of each. [b]The membranes were prepared with ZIF-67 membranes hydrothermally treated in an aqueous ligand solution before tertiary growth of a ZIF-8 layer or a ZIF-67 layer.

tested membranes. ZIF-67 membranes exhibit the average propylene permeance of ~460 × 10^{-10} mol Pa^{-1} m^{-2} s^{-1} and the average propylene/propane separation factor of ~85, outperforming almost all of the reported ZIF-8 membranes (Table S2). This impressive binary propylene/propane separation performance of ZIF-67 membranes is ascribed to their submicron thickness (ca. 700 nm) and improved grain boundary structure. Since the performance of high-quality polycrystalline membranes is determined not only by the quality of grain boundary structure (i.e., nonselective intercrystalline diffusion) but also by the intrinsic transport property of materials (i.e., selective intracrystalline diffusion); however, it is not feasible to exclude the possibility that ZIF-67 might be inherently better than ZIF-8 for propylene/propane separation. While the crystallographically determined pore apertures show negligible difference between ZIF-8 and ZIF-67 (Table S1), the IR band corresponding to the metal−nitrogen stretching frequency in ZIF-67 (ν_{Co-N}) is blue-shifted as compared to the one in ZIF-8 (ν_{Zn-N}) (Figure 4a). This blue shift implies that Co−N bonds are more rigid (i.e., stiffer connectivity) than Zn−N bonds. Figure 4b,c compares the ^{13}C and ^{15}N NMR spectra of ZIF-8 and ZIF-67. The resonance peaks of ZIF-67 are notably downshifted when compared to ZIF-8, which is attributed to the higher electronegativity of cobalt than zinc (1.88 (cobalt) vs 1.65 (zinc)). This implies that Co−N bonds are more ionic than Zn−N bonds, and are therefore stiffer, consistent with the IR results. Furthermore, both of the ^{13}C and ^{15}N NMR peaks of ZIF-67 are substantially broader than those of ZIF-8 primarily due to the shielding effect of the unpaired electrons of Co^{2+}.[59] Considering the fact that the effective pore aperture of ZIFs depends on the magnitude of ligand flipping motion,[60] it is not unreasonable to surmise that the more rigid the metal−nitrogen connectivity is, the less the degree of the ligand flipping motion is. This restricted motion might lead to the slightly smaller effective pore aperture of ZIF-67 and consequently improved separation factors. At this point, it is worth mentioning that our attempts to determine the diffusion coefficients of propylene and
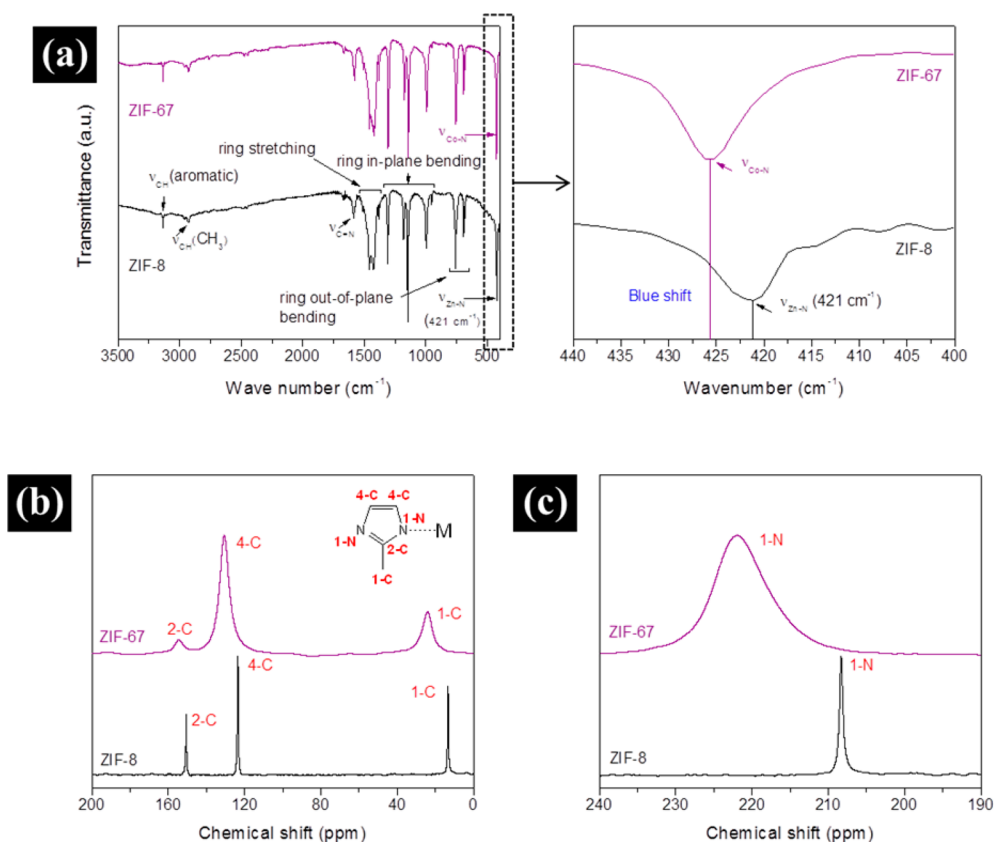
Figure 4. FT-IR (a) and ^{13}C (b) and ^{15}N (c) NMR spectra of ZIF-8 and ZIF-67 powders.

propane in ZIF-67 using kinetic sorption measurements failed to lead to any meaningful data (not shown here) mainly owning to (1) the insufficient size of ZIF-67 crystals (short diffusion time scale) and (2) the rather wide size distribution. Further studies on the measurement of diffusion coefficients using PFG-NMR[61] and IR microimaging[62] are, however, essential and currently underway in collaborations to elucidate the mechanisms by which ZIF-67 membranes perform better than ZIF-8 membranes.

The presence of an organic solvent (methanol) in an aqueous precursor solution was found to be critical to ensure the quality and reproducibility of ZIF-67 membranes. In the absence of methanol, the membranes not only grew thicker (1.8 μm) (Figure S12) but also formed visible white spots containing pinhole defects in an uncontrolled manner (Figure S13). These ZIF-67 membranes show comparatively low permeance and poor reproducibility in general as shown in Table S3.

Propylene/Propane Separation Performances of ZIF-8/ZIF-67 Membranes. Interestingly, remarkable enhancement in the propylene/propane separation factors was observed upon the addition of a ZIF-8 overlayer (~300 nm) on ZIF-67 membranes by tertiary growth (Table 1 and Figure S14a). The average propylene/propane separation factor of ~190 was obtained after 2 h of the measurement. As shown in Figure 5a, however, the propylene permeance gradually decreases as the measurement time increases, consequently resulting in the decrease in propylene/propane separation factors, approximately 36% and 38% reduction in the permeance and separation factor, respectively, after 70 h of the on-stream measurement. In contrast, both ZIF-8 and ZIF-67 membranes showed relatively stable performances throughout the measure-

ments (Figure S15). X-ray diffraction patterns of the membranes before and after the measurement indicate that the overall crystallinity of the samples was preserved (Figure S16). Furthermore, N_2 adsorption measurements on ZIF-8 and ZIF-67 powder samples show no appreciable pore structure change after being exposed to the propylene/propane mixture stream over 5 days (Figure S17). Since both X-ray diffraction and N_2 adsorption analyses give average structural information, however, it is not possible to rule out the local structure change during the permeation measurements. It is our hypothesis that local defects such as under-saturated metal (Co) sites[63−65] might have been generated during the heteroepitaxial tertiary growth of the ZIF-8 overlayer and the local structure might have been modified during the measurements, causing the performance instability.

By treating a secondarily grown ZIF-67 layer hydrothermally with an aqueous ligand solution prior to the tertiary growth of a ZIF-8 overlayer, the performance of ZIF-8/ZIF-67 membranes was stabilized (Figure 5b). Notably, after the ligand treatment, the propylene permeance amounted to ~370 × 10^{-10} mol Pa^{-1} m^{-2}s^{-1} while the propylene/propane separation factors remained high (~200). The propylene/propane separation factor of ~200 is unprecedented. The ligand treatment neither compromised the crystallinity of the ZIF-67 layer nor changed the thickness of final ZIF-8/ZIF-67 membranes (Figure S18). It is hypothesized that the surface defects of ZIF-67 layers were likely healed during hydrothermal ligand treatment, minimizing defect sites possibly at the interface between ZIF-8 and ZIF-67 layers as well as at the grain boundary, thereby stabilizing the membrane performance. ^{13}C NMR spectra of ZIF-67 powders (Figure S19) revealed peak sharpening after the ligand
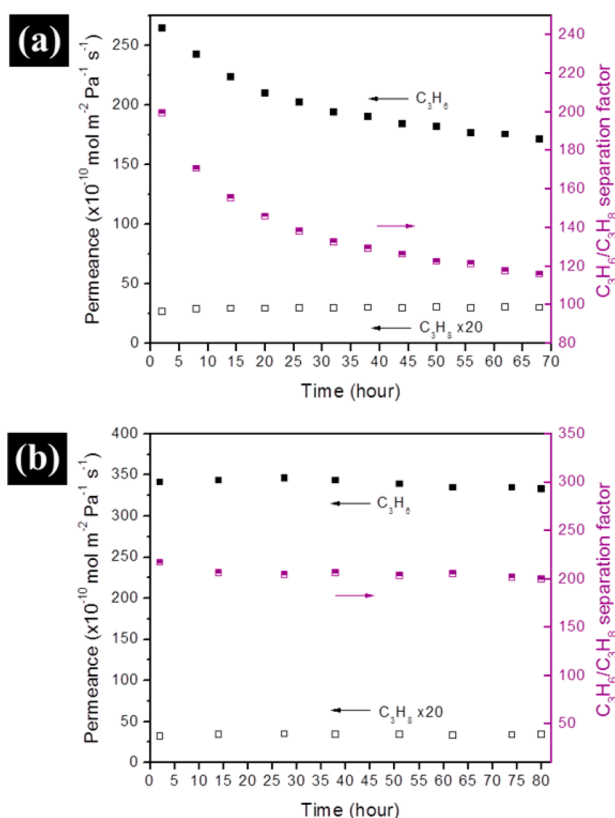
Figure 5. On-stream propylene/propane separation performances of ZIF-8/ZIF-67 membranes with ZIF-67 layers (a) before and (b) after hydrothermal ligand treatment prior to the tertiary growth of a ZIF-8 layer.

treatment, implying the increased uniformity of carbon environments due to reduced defect sites.

Lastly, it was found that this ligand treatment/tertiary growth effect (i.e., enhancing and stabilizing membrane performance) was not specific to ZIF-8 overlayers as verified by ZIF-67/ZIF-67 membranes (i.e., ZIF-67 membranes with ZIF-67 overlayers) exhibiting not only enhancement in the separation factors but also stabilization in the membrane performance (see Table 1 and Figure S20). It should be noted that ZIF-67/ZIF-67 membranes showed a much larger sample-to-sample variation than ZIF-8/ZIF-67 membranes. This result implies that the grain boundary structure of ZIF-67 membranes was further improved due to the tertiary growth of overlayers (whether ZIF-8 or ZIF-67). Improved grain boundary structure alone might not account for the significantly enhanced separation performance (from ~85 to ~200), given the expected propylene/propane diffusion separation factor 125−145.[24,58] It is reasonable to expect that the selective intracrystalline transport pathway of ZIF-67, which might be inherently better than that of ZIF-8 as hypothesized and discussed earlier, became more important than the nonselective intercrystalline pathway (i.e., transport through grain boundary), thereby resulting in dramatic increase of propylene/propane separation performance. In other words, as the intercrystalline transport resistance becomes larger, the intracrystalline transport resistance becomes more important for the overall resistance in the resistances-in-parallel model. Furthermore, forming ZIF-8 overlayers on ZIF-8 membranes by the tertiary growth did not result in as much improvement as ZIF-67 membranes (not shown here). These observations

strengthen our hypothesis that ZIF-67 might be inherently more propylene-selective than ZIF-8.

Performance Comparison. Lastly, Figure 6 compares the propylene/propane separation performances of our ZIF
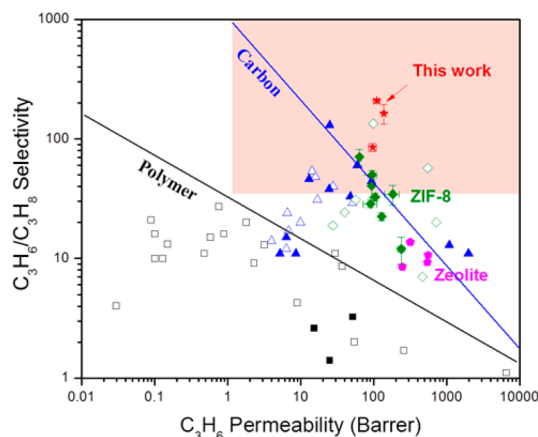

Figure 6. Comparison of the propylene/propane separation performances with previously reported membranes. Open and closed symbols denote separation data obtained from single and binary gas permeation tests, respectively: rectangle, polymer membranes;[2] triangle, carbon membranes;[3−6] pentagon, zeolite membranes;[7] rhombus, ZIF-8 membranes;[8,25−32] star, this work.

membranes with those membranes previously reported. As shown in the figure, our membranes satisfy the proposed performance criteria[66] (a minimum permeability of 1 Barrer and selectivity of 35) for commercial applications. More importantly, both of our ZIF-67 and ZIF-8/ZIF-67 membranes significantly outperform polymer and carbon molecular sieve membranes as well as polycrystalline membranes such as zeolite and ZIF-8.

■ CONCLUSION

Here, for the first time, we have successfully applied the heteroepitaxial growth to prepare well-intergrown ZIF-67 and ZIF-8/ZIF-67 membranes displaying exceptional propylene/propane separation performance. The heteroepitaxial growth between ZIF-8 and ZIF-67 was unambiguously determined. Strongly attached and densely packed ZIF-8 seed crystals were found to be essential to heteroepitaxially prepare ZIF-67 membranes. In addition, the presence of a methanol cosolvent in the ZIF-67 secondary growth solution led to the reduction in the membrane thickness as well as to the enhancement in the reproducibility. The resulting submicron thick ZIF-67 membranes displayed an outstanding binary propylene/propane separation performance (average propylene permeance of ~460 × 10⁻¹⁰ mol Pa⁻¹ m⁻² s⁻¹ and average separation factor of ~85), outperforming almost all of the previously reported ZIF-8 membranes. Furthermore, the tertiary heteroepitaxial growth of ZIF-8 layers on ZIF-67 membranes stabilized by hydrothermally treating in a ligand solution resulted in an unprecedentedly high propylene/propane separation factor of ~200. Heteroepitaxially grown ZIF membranes with remarkable propylene/propane separation performances are a significant step forward for bringing membrane-based propylene/propane separation close to the commercial applications.

■ ASSOCIATED CONTENT

S Supporting Information

The Supporting Information is available free of charge on the ACS Publications website at DOI: 10.1021/jacs.5b06730.

Figures S1−S20, Tables S1−S3, and experimental procedures (PDF)

ZIF-8 single crystal structure data (CIF)

ZIF-67 single crystal structure data (CIF)

■ AUTHOR INFORMATION

Corresponding Author

*hjeong7@tamu.edu

Notes

The authors declare no competing financial interest.

■ ACKNOWLEDGMENTS

■ REFERENCES

(1) Baker, R. W. *Ind. Eng. Chem. Res.* **2002**, *41*, 1393.

(2) Burns, R. L.; Koros, W. J. *J. Membr. Sci.* **2003**, *211*, 299.

(3) Chng, M. L.; Xiao, Y.; Chung, T.-S.; Toriida, M.; Tamai, S. *Carbon* **2009**, *47*, 1857.

(4) Hayashi, J.-i.; Mizuta, H.; Yamamoto, M.; Kusakabe, K.; Morooka, S.; Suh, S.-H. *Ind. Eng. Chem. Res.* **1996**, *35*, 4176.

(5) Ma, X.; Lin, B. K.; Wei, X.; Kniep, J.; Lin, Y. S. *Ind. Eng. Chem. Res.* **2013**, *52*, 4297.

(6) Okamoto, K.-i.; Kawamura, S.; Yoshino, M.; Kita, H.; Hirayama, Y.; Tanihara, N.; Kusuki, Y. *Ind. Eng. Chem. Res.* **1999**, *38*, 4424.

(7) Nikolakis, V.; Xomeritakis, G.; Abibi, A.; Dickson, M.; Tsapatsis, M.; Vlachos, D. G. *J. Membr. Sci.* **2001**, *184*, 209.

(8) Kwon, H. T.; Jeong, H.-K. *J. Am. Chem. Soc.* **2013**, *135*, 10763.

(9) Takht Ravanchi, M.; Kaghazchi, T.; Kargari, A. *Desalination* **2009**, *235*, 199.

(10) Qiu, S.; Xue, M.; Zhu, G. *Chem. Soc. Rev.* **2014**, *43*, 6116.

(11) Shah, M.; McCarthy, M. C.; Sachdeva, S.; Lee, A. K.; Jeong, H.-K. *Ind. Eng. Chem. Res.* **2012**, *51*, 2179.

(12) Shekhah, O.; Liu, J.; Fischer, R. A.; Woll, C. *Chem. Soc. Rev.* **2011**, *40*, 1081.

(13) Park, K. S.; Ni, Z.; Côté, A. P.; Choi, J. Y.; Huang, R.; Uribe-Romo, F. J.; Chae, H. K.; O'Keeffe, M.; Yaghi, O. M. *Proc. Natl. Acad. Sci. U. S. A.* **2006**, *103*, 10186.

(14) Yao, J.; Wang, H. *Chem. Soc. Rev.* **2014**, *43*, 4470.

(15) Li, Y.; Liang, F.; Bux, H.; Yang, W.; Caro, J. *J. Membr. Sci.* **2010**, *354*, 48.

(16) Bux, H.; Liang, F.; Li, Y.; Cravillon, J.; Wiebcke, M.; Caro, J. *J. Am. Chem. Soc.* **2009**, *131*, 16000.

(17) Huang, A.; Bux, H.; Steinbach, F.; Caro, J. *Angew. Chem.* **2010**, *122*, 5078.

(18) Liu, Y.; Hu, E.; Khan, E. A.; Lai, Z. *J. Membr. Sci.* **2010**, *353*, 36.

(19) Dong, X.; Lin, Y. S. *Chem. Commun.* **2013**, *49*, 1196.

(20) Dong, X.; Huang, K.; Liu, S.; Ren, R.; Jin, W.; Lin, Y. S. *J. Mater. Chem.* **2012**, *22*, 19222.

(21) Huang, A.; Dou, W.; Caro, J. *J. Am. Chem. Soc.* **2010**, *132*, 15562.

(22) Huang, A.; Chen, Y.; Wang, N.; Hu, Z.; Jiang, J.; Caro, J. *Chem. Commun.* **2012**, *48*, 10981.

(23) Aguado, S.; Nicolas, C.-H.; Moizan-Basle, V.; Nieto, C.; Amrouche, H.; Bats, N.; Audebrand, N.; Farrusseng, D. *New J. Chem.* **2011**, *35*, 41.

(24) Zhang, C.; Lively, R. P.; Zhang, K.; Johnson, J. R.; Karvan, O.; Koros, W. J. *J. Phys. Chem. Lett.* **2012**, *3*, 2130.

(25) Kwon, H. T.; Jeong, H.-K. *Chem. Eng. Sci.* **2015**, *124*, 20.

(26) Kwon, H. T.; Jeong, H.-K. *Chem. Commun.* **2013**, *49*, 3854.

(27) Pan, Y.; Li, T.; Lestari, G.; Lai, Z. *J. Membr. Sci.* **2012**, *390−391*, 93.

(28) Liu, D.; Ma, X.; Xi, H.; Lin, Y. S. *J. Membr. Sci.* **2014**, *451*, 85.

(29) Hara, N.; Yoshimune, M.; Negishi, H.; Haraya, K.; Hara, S.; Yamaguchi, T. *J. Membr. Sci.* **2014**, *450*, 215.

(30) Brown, A. J.; Brunelli, N. A.; Eum, K.; Rashidi, F.; Johnson, J. R.; Koros, W. J.; Jones, C. W.; Nair, S. *Science* **2014**, *345*, 72.

(31) Hara, N.; Yoshimune, M.; Negishi, H.; Haraya, K.; Hara, S.; Yamaguchi, T. *Microporous Mesoporous Mater.* **2015**, *206*, 75.

(32) Hara, N.; Yoshimune, M.; Negishi, H.; Haraya, K.; Hara, S.; Yamaguchi, T. *J. Chem. Eng. Jpn.* **2014**, *47*, 770.

(33) Shah, M.; Kwon, H. T.; Tran, V.; Sachdeva, S.; Jeong, H.-K. *Microporous Mesoporous Mater.* **2013**, *165*, 63.

(34) Venna, S. R.; Carreon, M. A. *J. Am. Chem. Soc.* **2010**, *132*, 76.

(35) Wang, Z.; Cohen, S. M. *Chem. Soc. Rev.* **2009**, *38*, 1315.

(36) Burrows, A. D. *CrystEngComm* **2011**, *13*, 3623.

(37) Cubillas, P.; Anderson, M. W.; Attfield, M. P. *Chem. - Eur. J.* **2013**, *19*, 8236.

(38) Furukawa, S.; Hirai, K.; Nakagawa, K.; Takashima, Y.; Matsuda, R.; Tsuruoka, T.; Kondo, M.; Haruki, R.; Tanaka, D.; Sakamoto, H.; Shimomura, S.; Sakata, O.; Kitagawa, S. *Angew. Chem., Int. Ed.* **2009**, *48*, 1766.

(39) Furukawa, S.; Hirai, K.; Takashima, Y.; Nakagawa, K.; Kondo, M.; Tsuruoka, T.; Sakata, O.; Kitagawa, S. *Chem. Commun.* **2009**, 5097.

(40) Koh, K.; Wong-Foy, A. G.; Matzger, A. J. *Chem. Commun.* **2009**, 6162.

(41) Liu, B.; Tu, M.; Zacher, D.; Fischer, R. A. *Adv. Funct. Mater.* **2013**, *23*, 3790.

(42) Shekhah, O.; Hirai, K.; Wang, H.; Uehara, H.; Kondo, M.; Diring, S.; Zacher, D.; Fischer, R. A.; Sakata, O.; Kitagawa, S.; Furukawa, S.; Woll, C. *Dalton Trans.* **2011**, *40*, 4954.

(43) Shekhah, O.; Swaidan, R.; Belmabkhout, Y.; du Plessis, M.; Jacobs, T.; Barbour, L. J.; Pinnau, I.; Eddaoudi, M. *Chem. Commun.* **2014**, *50*, 2089.

(44) Szilagyi, P. A.; Lutz, M.; Gascon, J.; Juan-Alcaniz, J.; van Esch, J.; Kapteijn, F.; Geerlings, H.; Dam, B.; van de Krol, R. *CrystEngComm* **2013**, *15*, 6003.

(45) Tan, T. T. Y.; Cham, J. T. M.; Reithofer, M. R.; Andy Hor, T. S.; Chin, J. M. *Chem. Commun.* **2014**, *50*, 15175.

(46) Tu, M.; Fischer, R. A. *J. Mater. Chem. A* **2014**, *2*, 2018.

(47) Yoo, Y.; Jeong, H.-K. *Cryst. Growth Des.* **2010**, *10*, 1283.

(48) Jeong, H.-K.; Krohn, J.; Sujaoti, K.; Tsapatsis, M. *J. Am. Chem. Soc.* **2002**, *124*, 12966.

(49) Wakihara, T.; Yamakita, S.; Iezumi, K.; Okubo, T. *J. Am. Chem. Soc.* **2003**, *125*, 12388.

(50) Banerjee, R.; Phan, A.; Wang, B.; Knobler, C.; Furukawa, H.; O'Keeffe, M.; Yaghi, O. M. *Science* **2008**, *319*, 939.

(51) Llabrés i Xamena, F. X.; Casanova, O.; Galiasso Tailleur, R.; Garcia, H.; Corma, A. *J. Catal.* **2008**, *255*, 220.

(52) Tian, Y.-Q.; Cai, C.-X.; Ren, X.-M.; Duan, C.-Y.; Xu, Y.; Gao, S.; You, X.-Z. *Chem. - Eur. J.* **2003**, *9*, 5673.

(53) Lu, Y.; Tonigold, M.; Bredenkötter, B.; Volkmer, D.; Hitzbleck, J.; Langstein, G. *Z. Anorg. Allg. Chem.* **2008**, *634*, 2411.

(54) Beier, M. J.; Kleist, W.; Wharmby, M. T.; Kissner, R.; Kimmerle, B.; Wright, P. A.; Grunwaldt, J.-D.; Baiker, A. *Chem. - Eur. J.* **2012**, *18*, 887.

(55) Tonigold, M.; Lu, Y.; Bredenkötter, B.; Rieger, B.; Bahnmüller, S.; Hitzbleck, J.; Langstein, G.; Volkmer, D. *Angew. Chem., Int. Ed.* **2009**, *48*, 7546.

(56) Zakzeski, J.; Dębczak, A.; Bruijnincx, P. C. A.; Weckhuysen, B. M. *Appl. Catal., A* **2011**, *394*, 79.

(57) Tang, J.; Salunkhe, R. R.; Liu, J.; Torad, N. L.; Imura, M.; Furukawa, S.; Yamauchi, Y. *J. Am. Chem. Soc.* **2015**, *137*, 1572.

(58) Li, K.; Olson, D. H.; Seidel, J.; Emge, T. J.; Gong, H.; Zeng, H.; Li, J. *J. Am. Chem. Soc.* **2009**, *131*, 10368.

(59) Kuttatheyil, A. V.; Lässig, D.; Lincke, J.; Kobalz, M.; Baias, M.; König, K.; Hofmann, J.; Krautscheid, H.; Pickard, C. J.; Haase, J.; Bertmer, M. *Inorg. Chem.* **2013**, *52*, 4431.

(60) Zheng, B.; Pan, Y.; Lai, Z.; Huang, K.-W. *Langmuir* **2013**, *29*, 8865.

(61) Mueller, R.; Kanungo, R.; Kiyono-Shimobe, M.; Koros, W. J.; Vasenkov, S. *Langmuir* **2012**, *28*, 10296.

(62) Chmelik, C. *Microporous Mesoporous Mater.* **2015**, *216*, 138.

(63) Tian, F.; Cerro, A. M.; Mosier, A. M.; Wayment-Steele, H. K.; Shine, R. S.; Park, A.; Webster, E. R.; Johnson, L. E.; Johal, M. S.; Benz, L. *J. Phys. Chem. C* **2014**, *118*, 14449.

(64) Chizallet, C.; Lazare, S.; Bazer-Bachi, D.; Bonnier, F.; Lecocq, V.; Soyer, E.; Quoineaud, A.-A.; Bats, N. *J. Am. Chem. Soc.* **2010**, *132*, 12365.

(65) Chizallet, C.; Bats, N. *J. Phys. Chem. Lett.* **2010**, *1*, 349.

(66) Colling, C. W.; Huff, G. A.; Bartels, J. V. U.S. Patent 2004/0004040 A1, 2004.